Constitutive behaviour of confined fibre reinforced concrete under axial compression

K. Ramesh [a,b], D.R. Seshu [a,*], M. Prabhakar [b]

[a] *Department of Civil Engineering, Regional Engineering College, Warangal 506 004, Andhra Pradesh, India*
[b] *Department of Civil Engineering, KITS, Warangal 506 015, Andhra Pradesh, India*

Abstract

Steel fibre reinforced concrete is finding extensive use in field applications. The mechanism of delaying and arresting crack propagation by the fibres can be made use in passive confinement of concrete. Such concrete was termed as confined fiber reinforced concrete (CFRC). This paper presents an analytical model for predicting the stress–strain behaviour of CFRC based on the experimental results. A total of ninety prisms of size $150 \times 150 \times 300$ mm were cast and tested under strain control rate of loading. The increase in strength and strain of CFRC were used in formulating the constitutive relation.
© 2002 Elsevier Science Ltd. All rights reserved.

1. Introduction

The provision of adequate ductility in concrete structures has been engaging the attention of several researchers nowadays. The presence of micro-cracks at the mortar aggregate interface is responsible for the inherent weakness of plain concrete and results in poor ductility. This weakness can be rectified by the inclusion of the fibres in the mix. The fibres help to transfer loads at the internal micro-cracks. Such concrete is popularly known as fibre reinforced concrete (FRC). Thus, the FRC [1] is a composite material essentially consisting of concrete reinforced by random placement of short, discontinuous and discrete fine fibre of specific geometry. Several investigations [2–6] on FRC revealed that the inclusion of fibres enhanced many of structural properties of basic materials viz., fracture toughness, flexural strength, tensile strength, impact strength, resistance to fatigue and thermal shock. Essentially, the fibres acts as crack arresters, restricting the development of crack and thus transforming an inherently brittle matrix into a strong composite with better crack resistance and ductility. The inclusion of fibres delays the dilation of

concrete by acting as crack arresters and thus helps indirectly in confinement of concrete under compressive loads. Normal reinforced concrete may exhibit improved ductile characteristics due to direct and indirect confinement of concrete by lateral ties and fibres respectively. The FRC confined with laterals [7–10] was termed as confined fiber reinforced concrete (CFRC). The confinement provided by binders [11–14] depends on parameters such as spacing of binders, cross-sectional area of binder, strength of binder, strength of concrete, presence of main reinforcement (its type, amount and location etc.,) and shape of concrete core confined. All these parameters were taken in to consideration by specifying the confinement index (C_i) defined in earlier investigations [15], which quantifies the level of confinement provided by lateral ties. The reinforcing index (RI), a product of weight fraction and aspect ratio of fibres was used in quantifying the strength of FRC [16]. An understanding of the deformability of CFRC is necessary for computing deformation of structures with CFRC provided at critical sections and to compute the stresses from observed strain. In the present investigation, the combined effect of C_i and RI was studied from the point of deformability characteristics of CFRC. A relation is proposed for constitutive behaviour of CFRC under axial compression.

---
* Corresponding author. Fax: +91-8712-459853.
E-mail address: drseshu@recw.ernet.in (D.R. Seshu).

Nomenclature

b, d	lateral dimensions of prism
f_y	yield strength of longitudinal/tie/fibre (Table 1)
A_s	area of longitudinal steel
f_c'	strength of unconfined concrete
ε_c'	strain at peak of unconfined concrete
f_{ct}	$f_c'(1 + 0.55C_i)$ = strength of tie confined concrete [15]
ε_{ct}	$\varepsilon_c'(1 + 5.2C_i)$ = strain at peak of tie confined concrete [15]
A_g	gross cross-sectional area
W_f	weight fraction = ratio of weight of steel fibre and weight of concrete
C_i	confinement index = $(P_b - P_{bb})(\frac{f_v}{f_c'})\sqrt{b/s}$
P_b	ratio of volume of transverse steel to the volume of concrete
P_{bb}	ratio of volume of transverse steel to the volume of concrete corresponding to a limiting pitch equal to 1.5b
f_v	stress in the lateral ties = $E_s\varepsilon_v$
ε_v	$0.0015 + 0.00076(P_b - P_{bb})\sqrt{b/s}$ = strain in the steel binder [15]
s	spacing of ties
ε_u	strain at peak of CFRC
$\varepsilon_{0.85u}$	strain at 85% of peak of CFRC in the descending portion of stress–strain curve
f_u	peak strength of CFRC
nd	neutral axis depth
C_f	compression force in CFRC under bending
M_c	moment of C_f about neutral axis
f	compressive stress in CFRC section
ε	compressive strain in CFRC section
RI	reinforcing index = product of weight fraction of fibre (W_f) and aspect ratio of fiber
ε_c	extreme compressive strain in CFRC section under bending
f_c	extreme compressive stress in CFRC section under bending
K	load factor explained in Table 2

2. Experimental programme

2.1. Scheme of experimental work

The experimental programme was designed to study the behaviour of confined steel FRC under axial compression by testing prisms of size 150 mm × 150 mm × 300 mm. The variables in the study are reinforcing index (RI) of the steel fibre, which controls the behaviour of the FRC and confinement index (C_i) of lateral steel reinforcement [15], which indicates the degree of confinement provided by laterals.

The programme consisted of casting and testing 90 prisms, which were cast in two groups. The first group of prisms cast with M20 grade of concrete and second with M25 grade of concrete. Each group was cast in five batches. The prisms in each batch were divided into three sets. In each set three identical specimens were cast and tested and the average behaviour was taken to represent the behaviour for that set of three specimens. Hence in each batch the total number of prisms amounted to nine.

Out of three sets of group I category (A, B and C) in each batch, the first set consisted of two lateral ties ($C_i = 0.0$) second sets consisted of five lateral ties ($C_i = 0.30$) and third consisted of seven lateral ties ($C_i = 0.56$). And in the three sets group II category (D, E and F) in each batch, the first set consisted of two lateral ties ($C_i = 0.0$), second set consisted of four lateral ties ($C_i = 0.08$) and third set consisted of seven lateral ties ($C_i = 0.19$).

Each group, out of five batches, the first batch with 0% (RI = 0.00) fibre, second batch with 0.30% (RI = 0.74) fibre, third batch with 0.6% (RI = 1.48) fibre, fourth batch with 0.9% (RI = 2.22) fibre and fifth batch with 1.20% (RI = 2.96) fibre were cast. Proper designation was given for each specimen. The details of prisms are given in Table 1.

2.2. Materials used

0.5 mm diameter steel fibres with aspect ratio 75 were used in all the specimens. 3.9 mm and 3 mm diameter G.I. wire are used as longitudinal reinforcement in group I and group II respectively. Lateral ties used were mild steel. The cement used was 43 grade conforming to IS sieve was used. M20 and M25 grade of concretes were used for group I and group II respectively throughout the work. The mix proportions adopted for M20 concrete 1:1.56:2.81 with water cement ratio 0.55 and for M25 concrete was 1:1.65:2.20 with water cement ratio 0.5.

2.3. Preparation of specimen

The ties were tied to the longitudinal bars at the required pitch in such a manner that the hooks were distributed evenly on all the four corners. Fig. 1 shows the reinforcement details of the specimen.

Table 1
Details of prisms

Sl. no.	Specimen designation	Longitudinal reinforcement		Lateral reinforcement				Steel fibre		f_c' (MPa)	$\varepsilon_c' \times 10^{-6}$
		Dia (mm)	f_y (MPa)	Dia (mm)	f_y (MPa)	Spacing (mm)	C_i	V_f (%)	RI		
1	A1	3.92	295	7.18	350	290	0.0	0	0	23.3	2100
2	B1	3.92	295	7.18	350	70	0.30	0	0	23.3	2100
3	C1	3.92	295	7.18	350	50	0.56	0	0	23.3	2100
4	A2	3.92	295	7.18	350	290	0.0	0.3	0.74	22.9	2050
5	B2	3.92	295	7.18	350	70	0.30	0.3	0.74	22.9	2050
6	C2	3.92	295	7.18	350	50	0.56	0.3	0.74	22.9	2050
7	A3	3.92	295	7.18	350	290	0.0	0.6	1.48	23.1	2075
8	B3	3.92	295	7.18	350	70	0.30	0.6	1.48	23.1	2075
9	C3	3.92	295	7.18	350	50	0.56	0.6	1.48	23.1	2075
10	A4	3.92	295	7.18	350	290	0.0	0.9	2.22	23.4	2125
11	B4	3.92	295	7.18	350	70	0.30	0.9	2.22	23.4	2125
12	C4	3.92	295	7.18	350	50	0.56	0.9	2.22	23.4	2125
13	A5	3.92	295	7.18	350	290	0.0	1.2	2.96	23.0	2000
14	B5	3.92	295	7.18	350	70	0.30	1.2	2.96	23.0	2000
15	C5	3.92	295	7.18	350	50	0.56	1.2	2.96	23.0	2000
16	D1	3.00	350	7.00	448	290	0.00	0.0	0.0	36.8	2020
17	E1	3.00	350	7.00	448	88	0.08	0.0	0.0	36.8	2020
18	F1	3.00	350	7.00	448	57	0.19	0.0	0.0	36.8	2020
19	D2	3.00	350	7.00	448	290	0.00	0.3	0.74	37.0	1980
20	E2	3.00	350	7.00	448	88	0.08	0.3	0.74	37.0	1980
21	F2	3.00	350	7.00	448	57	0.19	0.3	0.74	37.0	1980
22	D3	3.00	350	7.00	448	290	0.00	0.6	1.48	37.2	2010
23	E3	3.00	350	7.00	448	88	0.08	0.6	1.48	37.2	2010
24	F3	3.00	350	7.00	448	57	0.19	0.6	1.48	37.2	2010
25	D4	3.00	350	7.00	448	290	0.00	0.9	2.22	36.5	1970
26	E4	3.00	350	7.00	448	88	0.08	0.9	2.22	36.5	1970
27	F4	3.00	350	7.00	448	57	0.19	0.9	2.22	36.5	1970
28	D5	3.00	350	7.00	448	290	0.00	1.2	2.96	36.9	1990
29	E5	3.00	350	7.00	448	88	0.08	1.2	2.96	36.9	1990
30	F5	3.00	350	7.00	448	57	0.19	1.2	2.96	36.9	1990

Fig. 1. (a) Reinforcement details in prisms. (b) Moulds used for casting the prisms.

2.4. Casting of specimen

The prepared cage of reinforcement was kept in moulds carefully. The prisms were cast in the vertical position. First mould was filled to about the half height and then a needle vibrator was used to compact the core concrete. The mould was filled in three layers in the same technique. The top face of the prism specimen was decoupled 24 h after casting and cured for 28 days in the water.

2.5. Testing

The cured specimens were capped with plaster of Paris before testing to provide a smooth loading surface, to avoid any stress concentration during the application of load. A Tinius–Olsen testing machine of 1810 kN capacity was used for testing the prisms under axial compression. The prisms were tested under strain rate control, 0.1 mm/min. From the studies of previous investigators, who worked on the concrete confined with ties, it was observed that the cover concrete started spalling off about 90% of the ultimate load. Along the concrete, the resistance strain gauges and demec points
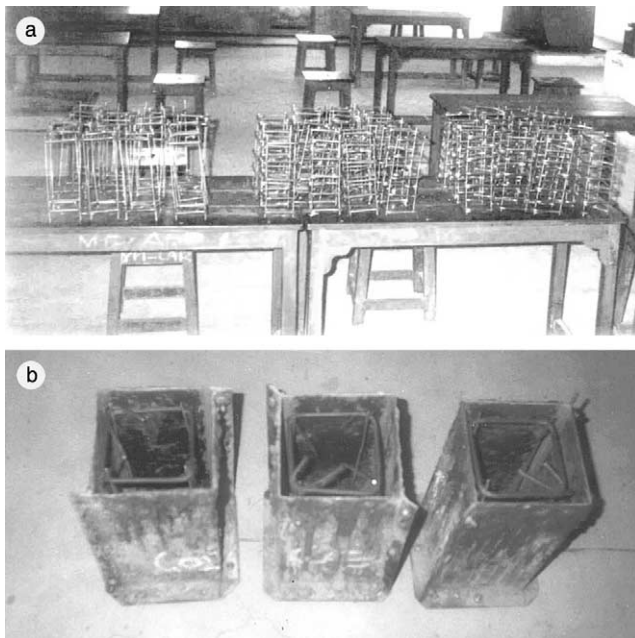
fixed to the concrete surface usually came off. Also the compressometer designed to measure the strains in standard concrete cylinders could not be fit to the square prisms.

To overcome the above-mentioned difficulties, compressometer suitable to prisms, which were fabricated by earlier investigators on confined concrete, were adopted. Each compressometer consisted of two square frames, a top frame and a bottom frame made of 12 mm square mild steel bars. Each frame was attached to the concrete specimen by two diametrically opposite pairs of screws at four points. The two frames were attached to the specimen symmetrically at the required gauge length, i.e., 150 mm apart two pairs of diametrical opposite dial gauges with a minimum count of 0.002 mm were attached to vertical hanger bars fixed to the top frame. The movable spindles of dial gauges rested on the plane circular heads of the adjustable screws, which were positioned in mild steel plates projecting frame was attached to the concrete specimen by two diametrically opposite pairs of screws at four points. The two frames were attached to the specimen symmetrically at the required gauge length, i.e., 150 mm apart two pairs of diametrical opposite dial gauges with a minimum count of 0.002 mm were attached to vertical hanger bars fixed to the top frame. The movable spindles of dial gauges rested on the plane circular heads of the adjustable
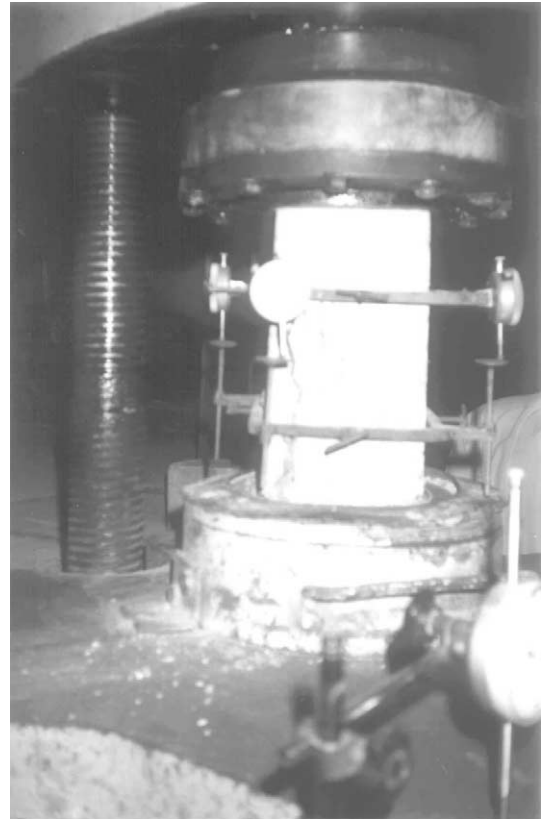

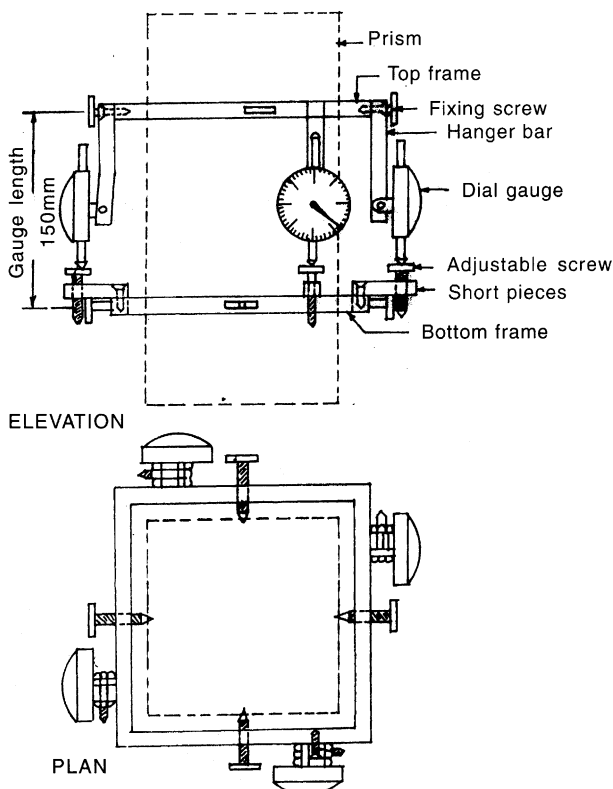Fig. 3. Compressometer attached to the prism.

Fig. 2. Details of compressometer.

screws, which were positioned in mild steel plates projecting horizontally from the bottom frame. The frames were attached to the specimen by means of screws, which would fit snugly to the concrete. Fig. 2 shows the details of the compressometer attached to the specimen. Fig. 3 shows the photograph of the same arrangement. The capped specimens with the compressometer attached were placed on the movable cross-head of the testing machine and tested under strain rate control. The deformations were noted and strains were calculated. The test was continued until the load dropped to about 75–80% of the ultimate load in the post ultimate region for both confined and unconfined concrete specimens.

3. Behaviour of CFRC

In the case of CFRC specimens, fine vertical cracks appeared on the surface of the specimen at about 75–80% of the peak load with increase of load, the number of cracks increased at a reduced rate compared to that of the confined reinforced concrete specimens. Beyond the peak load, the fine vertical cracks widened. The extent of the cracking and rate of decrease of the load after peak (in the descending portion of stress–strain curve) depended upon the reinforcing index (RI) of the fibre if the

Table 2
Test results of CFRC prisms

Sl. no.	Specimen designation	C_i	RI	P (kN)	K	ε_u ($\times 10^{-6}$)	$\varepsilon_u/\varepsilon_{ct}$	$\varepsilon_{0.85u}$ ($\times 10^{-6}$)	$\varepsilon_{0.85u}/\varepsilon_u$
1	A1	0.00	0.00	540.00	1.00	2000	1.0	3300	1.65
2	A2	0.00	0.74	600.75	1.14	2470	1.24	5250	2.13
3	A3	0.00	1.48	641.25	1.21	2850	1.43	6000	2.11
4	A4	0.00	2.22	671.63	1.25	3300	1.65	8250	2.50
5	A5	0.00	2.96	735.75	1.39	3820	1.91	9000	2.36
6	B1	0.30	0.00	614.25	0.98	4950	0.97	11100	2.24
7	B2	0.30	0.74	648.00	1.06	6000	1.17	13870	2.31
8	B3	0.30	1.48	680.85	1.14	7050	1.37	16200	2.30
9	B4	0.30	2.22	749.25	1.20	8250	1.61	20250	2.46
10	B5	0.30	2.96	830.25	1.35	9300	1.82	20850	2.24
11	C1	0.56	0.00	681.75	0.97	7800	0.99	16570	2.13
12	C2	0.56	0.74	702.00	1.02	9450	1.21	21000	2.22
13	C3	0.56	1.48	769.50	1.11	10500	1.34	21750	2.07
14	C4	0.56	2.22	810.00	1.16	12000	1.53	24250	2.02
15	C5	0.56	2.96	857.25	1.25	14050	1.80	29250	2.08
16	D1	0.00	0.00	866.25	1.03	1600	1.00	2100	1.31
17	D2	0.00	0.74	929.25	1.10	1800	1.13	2700	1.50
18	D3	0.00	1.48	1012.50	1.20	2200	1.38	3300	1.50
19	D4	0.00	2.22	1048.50	1.25	2250	1.41	3650	1.62
20	D5	0.00	2.96	1118.30	1.33	2500	1.56	3950	1.58
21	E1	0.08	0.00	960.75	1.09	2100	1.00	3750	1.78
22	E2	0.08	0.74	1014.90	1.16	2300	1.10	4350	1.89
23	E3	0.08	1.48	1077.80	1.23	2700	1.29	5100	1.89
24	E4	0.08	2.22	1109.30	1.27	2750	1.31	6450	2.35
25	E5	0.08	2.96	1140.80	1.30	2800	1.33	6900	2.46
26	F1	0.194	0.00	983.25	1.06	2950	1.00	5800	1.97
27	F2	0.194	0.74	1077.80	1.16	3200	1.09	6300	1.97
28	F3	0.194	1.48	1140.80	1.23	3400	1.15	7600	2.24
29	F4	0.194	2.22	1172.30	1.26	3800	1.29	8200	2.16
30	F5	0.194	2.96	1228.50	1.32	4100	1.39	8500	2.07

P = experimental ultimate load of prisms; K = factor indicating the improvement in ultimate strength due to addition of steel fiber (indirect confinement of steel fibre) = $((P - A_s f_y)/f_{ct} A_g)$.

$f_{ct} = f_c'(1.0 + 0.55 C_i)$ = strength of tie confined concrete [15]; $\varepsilon_{ct} = \varepsilon_c'(1.0 + 5.2 C_i)$ = strain at ultimate strength of tie confined concrete [15].

tie confinement indicated by confinement index (C_i is same. The higher the RI, the lower is the rate of decrease of load and the extent of spalling. This may be due to the improvement of internal crack arresting mechanism, dimensional stability as well as integrity of the material caused by the presence of large volume fraction of the fibre present in the concrete. Also, the presence of fibres might have enhanced the core concrete failure strain and resulted in an improvement in the strength and ductility of CFRC. The experimental results of ultimate strength of CFRC, the corresponding strain and the strain at 85% of ultimate strength (post peak) are shown in Table 2.

The ultimate strength of CFRC, the corresponding strain and strain at 0.85 times the ultimate strength (after the peak) varied linearly with reinforcing index of the fibre [11] for the same level of tie confinement. The prediction equations [11] fit for the same are

$$P = f_c'(1 + 0.55 C_i)(1.0228 + 0.1024(\text{RI}))A_g + f_y A_s \quad (1)$$

$$\varepsilon_u = \varepsilon_c'(1 + 5.2 C_i)(0.9899 + 0.2204(\text{RI})) \quad (2)$$

$$\frac{\varepsilon_{0.85u}}{\varepsilon_u} = 1.8847 + 0.121(\text{RI}) \quad (3)$$

where, $C_i = (P_b - P_{bb})\left(\dfrac{f_v}{f_c'}\right)\sqrt{\dfrac{b}{s}}$

4. Stress–strain curve for CFRC

From the observed data for a given specimen, the longitudinal deformation was calculated from the average readings of the four dial gauges of the compressometer. As there is no severe spalling in CFRC specimens until the load dropped by about 20–25% of peak load, the specimen were treated dimensionally stable and hence the gross cross-sectional area is used in calculating the stress values. The stress–strain curves were drawn for the three companion specimens of a set with the same origin and the average curve was taken to represent the set. Such average curves for all the sets of a particular batch with a common origin are shown in Fig. 4. These strain curves show that the addition of fiber has no significant influence on the stress–strain relationship up to 60–80% of the peak load of control specimen (the specimen contained RI = 0.0). However, the influence of fibre addition on the peak strength and ductility is highly appreciable. This may be due to
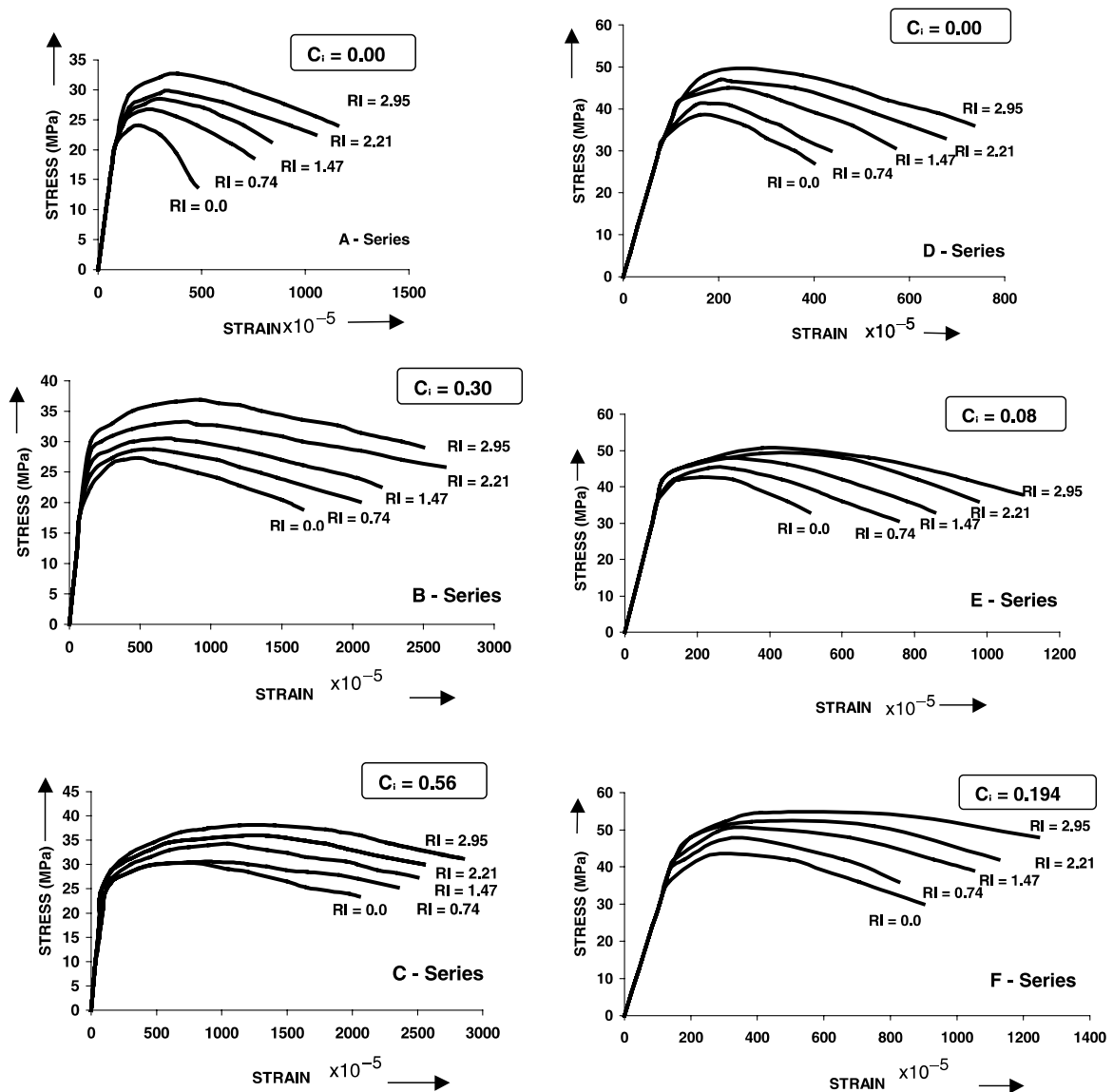
Fig. 4. Experimental stress–strain curves of tie confined frc prisms.

passive confinement to the core concrete due to improved the interfacial bond stresses between the core and cover concrete. This makes the cover and core concrete act as one unit in carrying the axial load and the resulting lateral strains. Such unification of the cover and the core concrete cannot be attained with the help of stirrups even if they are employed in a more sophisticated configuration. This conclusion is supported by the work conducted by Shah and Rangan [17]. They found that for the vertical spacing between the stirrups are greater than or equal to one half of the specimen dimension, the confinement provided by the laterals is negligible (i.e., $C_i = 0.0$) and for equal volumes of steels, fibres were superior to stirrups in improving ductility. This may be attributed to the fact that the fibres improve the integrity of all cross-sections along the height of the prism, whereas the stirrups provide confinement only to part of the core concrete at the tie or stirrup level, less confinement at other sections and least being at the section midway between the ties and no confinement whatsoever to the cover concrete.

An examination of the stress–strain diagrams for CFRC indicates that the behaviour is similar for all specimens. The similarity leads to the conclusion that there is a unique shape of the stress–strain diagram, if expressed in non-dimensional form, along both axes. The said form is obtained by dividing the stress at any level by the stress at ultimate and the strain at any stress level by the strain at ultimate. By non-dimensionalising the stress and strain as above the influence of reinforcing index (RI) and confinement index (C_i) is eliminated for any specimen. Fig. 5 shows the plot of characteristic
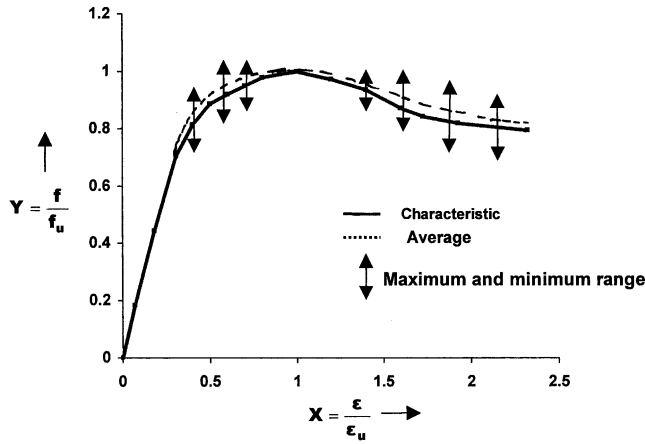
Fig. 5. Stress ratio (f/f_u) vs. strain ratio ($\varepsilon/\varepsilon_u$).

value of non-dimensionalised stress (stress ratio) as ordinate and non-dimensionalised strain (strain ratio) as abscissa. The plot indicates that the stress–strain behaviour of CFRC can be represented by a general curve, which functions as a stress block.

The following equation is fit for the non-dimensionalised characteristic stress–strain curve for CFRC in axial compression.

$$\frac{f}{f_u} = \left[\frac{A_1\left(\frac{\varepsilon}{\varepsilon_u}\right)}{1.0 + B_1\left(\frac{\varepsilon}{\varepsilon_u}\right) + C_1\left(\frac{\varepsilon}{\varepsilon_u}\right)^2} \right] \qquad (4)$$

where, for ascending portion of the stress–strain curve of CFRC: $A_1 = 2.1128$, $B_1 = 0.1128$, $C_1 = 1.0$; for descending portion of the stress–strain curve of CFRC: $A_1 = 1.6333$, $B_1 = -0.3666$, $C_1 = 1.0$.

Two sets of constants are proposed because the ascending portion of stress–strain curves i.e., beyond ultimate portion a slow downward trend. The common boundary conditions used are

(i)   At $\left(\frac{\varepsilon}{\varepsilon_u}\right) = 1.0$, $\left(\frac{f}{f_u}\right) = 1.0$ $\qquad (5)$

(ii) At $\left(\frac{\varepsilon}{\varepsilon_u}\right) = 1.0$, $\dfrac{\mathrm{d}\left(\frac{f}{f_u}\right)}{\mathrm{d}\left(\frac{\varepsilon}{\varepsilon_u}\right)} = 0.0$ $\qquad (6)$

Additional boundary conditions for ascending portion of stress–strain curve is

(iii) At $\left(\frac{\varepsilon}{\varepsilon_u}\right) = 0.3$, $\left(\frac{f}{f_u}\right) = 0.564$ $\qquad (7)$

For descending portion of stress–strain curve

(iv) At $\left(\frac{\varepsilon}{\varepsilon_u}\right) = 1.7$, $\left(\frac{f}{f_u}\right) = 0.85$ $\qquad (8)$

The condition (iii) and (iv) are obtained from the experimental data. At $(\varepsilon/\varepsilon_u) = 0.3$, the curve deviates from the initial tangent and at $(\varepsilon/\varepsilon_u) = 1.7$, the reduction in strength is 15%. The Fig. 6 indicates that the curve of the equation proposed passes close to all the experimental points.

Hence the generalized stress–strain equation for CFRC can be written as

$$f = \left[\frac{A\varepsilon}{1.0 + B\varepsilon + C\varepsilon^2} \right] \qquad (9)$$

where

$$A = A_1\left(\frac{f_u}{\varepsilon_u}\right), \quad B = B_1\left(\frac{1.0}{\varepsilon_u}\right), \quad C = C_1\left(\frac{1.0}{\varepsilon_u}\right)^2$$

The stress block parameters, useful in computing the ultimate moment of resistance and corresponding curvature of CFRC section, obtained using above proposed stress–strain equation as follows:
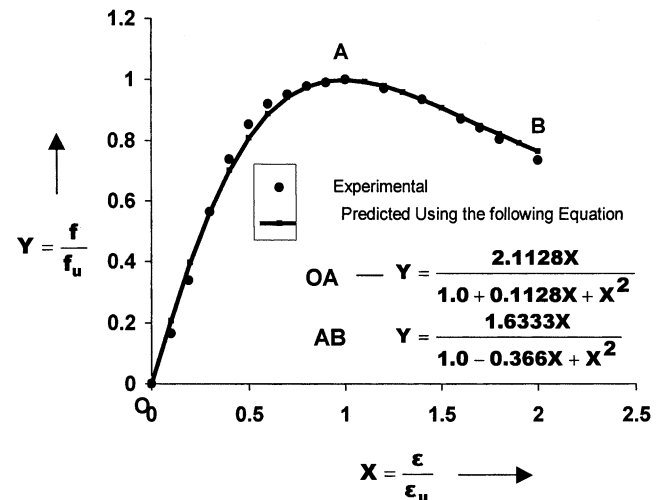
$$C_f = f_a bnd \qquad (10)$$

where,

$$f_a = \left(\frac{1.0}{\varepsilon_c}\right) \int_0^{\varepsilon_c} f \, \mathrm{d}\varepsilon \qquad (11)$$

$$M_c = b\left(\frac{nd}{\varepsilon_c}\right)^2 \int_0^{\varepsilon_c} f\varepsilon \, \mathrm{d}\varepsilon \qquad (12)$$

The evaluation of integrals $\int_0^{\varepsilon_c} f \, \mathrm{d}\varepsilon$ and $\int_0^{\varepsilon_c} f\varepsilon \, \mathrm{d}\varepsilon$ leads to the following expressions:

$$C_f = \frac{bnd}{\varepsilon_c}\left(\frac{A}{2C}K_1 - \frac{AB}{2C^2}K_2\right) \qquad (13)$$

Fig. 6. Characteristics stress ratio (f/f_u) vs. strain ration ($\varepsilon/\varepsilon_u$).

$$M_c = b \left(\frac{\text{nd}}{\varepsilon_c} \right)^2 \left\{ \frac{A}{C} \varepsilon_c - \frac{AB}{2C^2} K_1 + \frac{A}{2C^3} (B^2 - 2C) K_2 \right\} \tag{14}$$

where,

$$K_1 = \ln(1 + B\varepsilon_c + C\varepsilon_c^2) \tag{15}$$

K_2 will have three expressions depending on $(4C - B^2)$, as follows:

For $4C - B^2 < 0.0$ and $Q = \sqrt{(B^2 - 4C)}$;

$$K_2 = \frac{C}{Q} \ln \left\{ \frac{(2C\varepsilon_c + B - Q)(B + Q)}{(2C\varepsilon_c + B + Q)(B - Q)} \right\} \tag{16}$$

For $4C - B^2 = 0.0$;

$$K_2 = \frac{2A\varepsilon_c}{2C\varepsilon_c + B} \tag{17}$$

For $4C - B^2 > 0.0$ and $R = \sqrt{4C - B^2}$;

$$K_2 = \frac{2C}{R} \tan^{-1} \left(\frac{R\varepsilon_c}{2 + B\varepsilon_c} \right) \tag{18}$$

The corresponding curvature can be obtained as

$$\text{Curvature} = \phi = \left(\frac{\varepsilon_c}{\text{nd}} \right) \tag{19}$$

5. Conclusions

The following conclusions can be drawn from the experimental investigation on CFRC:

1. Steel fibre addition to tie CFRC specimens has the advantage over the confinement by lateral ties in improving the material properties, such as integrity, dimensional stability and performance under large deformations.
2. The non-dimensional characteristic equation proposed in this investigation can be used to predict the constitutive behaviour of CFRC in axial compression with reasonable accuracy.
3. The ultimate moment and corresponding curvature of the CFRC section can be determined by using the stress block parameters arrived at in this investigation.

4. Steel fibre addition to the tie confined reinforced concrete specimens provides indirect additional confinement of concrete in axial compression.

References

[1] Swamy RN, Mangat PS, Rao CVSK. The mechanism of fibre reinforcement of cement matrices. SP 44, American Concrete Institute, Detroit, 1974. p. 1–28.
[2] Balaguru N, Shah SP. Fibre reinforced cement composites. Singapore: McGraw Hill International Edition; 1992.
[3] Chen W, Carson JL. Stress–strain properties of random wire reinforced concrete. ACI J 1971;68(12):933–6.
[4] Fanella DA, Naaman AE. Stress–strain properties of fibre reinforced mortar in compression. ACI J 1985;82:475–83.
[5] Ramakrishnan V. Materials and properties of fibre reinforced concrete. In: Proceedings of International Symposium on Fibre Reinforced Concrete, vol. 1. Madras, India: SERC; 1987. p. 2.3–2.23.
[6] Mansur MA, Chin MS, Wee TH. Stress–strain relationship of confined high strength plain and fibre concrete. J Mater Civil Eng 1997;51(05):353–63.
[7] Alsayed SH. Confinement of reinforced concrete columns by rectangular ties and steel fibre. Mag Concr Res 1992;44(161):265–90.
[8] Ganesan N, Ramanamurthy JV. Strength and behaviour of confined steel fibre reinforced concrete columns. ACI Mater J 1990;87(03):221–3.
[9] Ramesh K, Seshu DR, Prabhakar M. A study of tie confined fibre reinforced concrete under axial compression. RILEM J Concr Sci Eng 2000;02:230–6.
[10] Ramesh K, Seshu DR, Prabhakar M. Confined fibre reinforced concrete (CFRC). In: Proceedings of 25th Anniversary International Conference on our World in Concrete and Structures Singapore. 2000. p. 531–6.
[11] Ahmed SH, Shah SP. Stress–strain curves of concrete confined by spiral reinforcement. ACI J Proc 1982;79(6):484–90.
[12] Baker ALL. The ultimate load theory applied to the design of reinforced and prestressed concrete frames. London: Concrete Publications Ltd; 1956.
[13] Rao AK, Reddy KN, Reddy VM. Effect of stirrup confinement on flexural behaviour of prestressed concrete simple beams. J IE (India) 1979;59:258–66.
[14] Sheikh AS. A comparative study of confinement models. ACI J Mater 1982;79(04):296–306.
[15] Reddy SR. Behaviour of concrete confined in rectangular binder and its application in flexure of reinforced concrete structures. PhD Thesis, J.T. University (India), 1974.
[16] Nataraja MC, Dhang N, Gupta AP. Steel fibre reinforced concrete under axial compression. Ind Concr J 1998:353–6.
[17] Shah SP, Rangan BV. Effects of reinforcements on ductility of concrete. Proc ASCE 1970;96(576):1167–84.